Production of Λ hyperons in 4 and 4.5 AGeV carbon-nucleus interactions at the Nuclotron

BM@N Collaboration

Abstract

The BM@N (Baryonic Matter at Nuclotron) is the first experiment undertaken at the accelerator complex of NICA-Nuclotron. The BM@N scientific program comprises studies of dense nuclear matter in heavy ion beams of the intermediate energy range between the SIS-18 and NICA/FAIR facilities. The first experimental run was performed in the carbon beam of the 4 and 4.5 AGeV kinetic energy with fixed targets. First physics results are presented on Λ hyperon production in carbon-nucleus interactions. Transverse momentum, rapidity spectra and yields of Λ hyperons are measured. The results are compared with predictions of theoretical models and with the experimental data on carbon-carbon interactions measured at lower energies.

1 Introduction

Collisions of relativistic heavy ions provide a unique opportunity to study nuclear matter at extreme densities and temperatures. At the Nuclotron with a beam kinetic energy per nucleon ranging from 1 to 4.5 GeV, baryons form the majority of the products in a nucleus-nucleus collision, in contrast to collisions that occur at higher energies at the RHIC or SPS accelerators. At the Nuclotron, the experimental research is focused on studies of hadrons with strangeness produced in the collision and not present in the initial state of two colliding nuclei, unlike the nucleons consisting of light (*u* and *d*) quarks. The energy range of ion beams at the Nuclotron corresponds to $\sqrt{s_{NN}} = 2.3 - 3.5$ GeV, these energies are high enough to study strange mesons and (multi)-strange hyperons produced in nucleus-nucleus collisions close to the kinematic threshold [4, 5].

BM@N (Baryonic Matter at Nuclotron) is the first experiment operational at the Nuclotron/ NICA accelerating complex. The purpose of the BM@N experiment is to study relativistic heavy ion beam interactions with fixed targets [7]. The Nuclotron will provide the experiment with beams of a variety of particles, from protons to gold ions, with a kinetic energy ranging from 1 to 6 GeV/nucleon for ions with Z/A ratio of 0.5. The maximum kinetic energy of gold ions with Z/A of 0.4 is 4.5 GeV/nucleon. Recently the BM@N experiment collected data in beams of carbon, argon, and krypton ions. This paper presents first results on Λ hyperon production in carbon-nucleus interactions. Transverse momentum, rapidity spectra and yields of Λ hyperons are measured. The results are compared with predictions of theoretical models and with the experimental data on carbon-carbon interactions measured at lower energies.

2 Experimental set-up

The experimental run of the BM@N detector was performed with the carbon beam in March 2017. The view of the BM@N setup used in the run is presented in Fig. 1. The experimental data from the central tracker, outer drift chambers (DCH), time-of-flight detectors (ToF), zero degree calorimeter (ZDC), trigger and T0 detectors (T0T) were read out using the integrated data acquisition system. The configuration of the central tracker was based on one plane of a forward silicon detector (Si) with double-side readout and six two-coordinate GEM (Gaseous Electron Multiplier) stations combined from 5 GEM detectors with the size of 66x41 cm^2 and 2 GEM detectors with the size of 163x45 cm^2 [6]. The tracking stations were arranged to have the beam passing through their centers. Each successive GEM station was rotated by 180^o around the vertical axis. It was done to have the opposite electron drift direction in the successive stations in order to avoid a systematic shift of reconstructed tracks due to the Lorentz angle in the magnetic field. The research program was devoted to measurements of inelastic reactions $C + A \to X$ with the beam kinetic energy of 4 and 4.5 AGeV and different targets: C, Al, Cu, Pb. The technical part of the run included the measurement of the carbon beam momentum and its resolution in the central and outer tracker at different values of the magnetic field. In addition, experimental data of minimum bias interactions of the beam with different targets were analyzed with the aim to reconstruct tracks, primary and secondary vertices using the central tracking detectors [8–10]. Since the GEM tracker configuration was tuned to measure relatively high-momentum beam particles, the geometric acceptance for relatively soft decay products of strange V0 (Λ, K^0_S) particles was rather low (few percent).

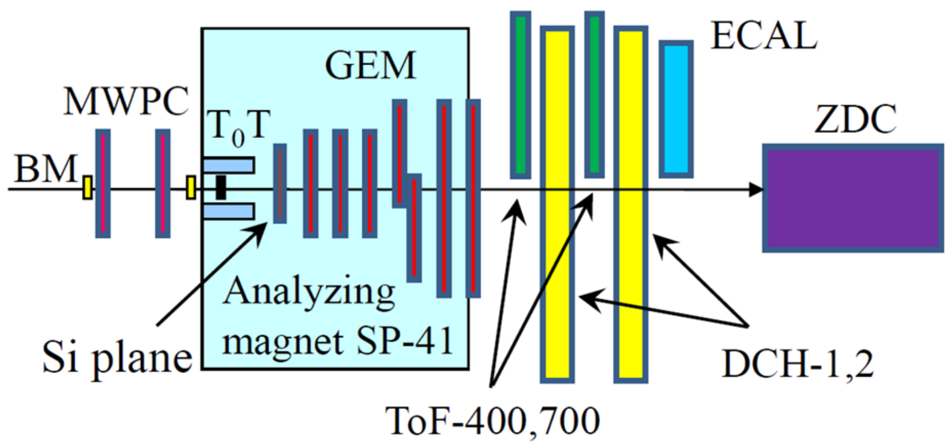

Figure 1: Scheme of the BM@N set-up in the carbon beam run.

In the present analysis the experimental data from the Forward Silicon detector, GEM detectors, trigger barrel multiplicity BD detector as well as beam, veto and T0 counters were used. The magnetic field in the center of the analyzing magnet was 0.61 T. The carbon beam intensity was few 10^5 per the spill, the spill duration was 2-2.5 sec. To form a minimum bias trigger signal a hit multiplicity in the barrel BD detector situated around the target was required to be $N_{BD} \geq 2$ for the carbon target and run dependent $N_{BD} \geq 2(3)$ for the Al, Cu, Pb targets.

The analysed statistics of carbon-nucleus collisions was 13M and 14M events for 4 AGeV and 4.5 AGeV carbon beam data, respectively.

3 Event reconstruction

The track reconstruction method was based on the so-called 'cellular automaton' approach [11] . Λ hyperons were reconstructed as V0 decay states using their decay mode into (p, π^-) pairs. Since particle identification at this stage of the analysis was not used, all positive tracks were considered as protons and all negative as π^-. Λ hyperon selection criteria were the following:

- Each track has at least 4 hits in Forward Silicon and GEM detectors (7 detectors in total), where hit is a combination of two strip clusters on both readout sides (X and X' views) on each detector [6]
- Momentum range of positive tracks is limited to $p_{pos} < 3.9(4.4)$ GeV/c for 4 (4.5) AGeV carbon beam data to remove tracks from the beam spot
- Momentum range of negative tracks: $p_{neg} > 0.3$ GeV/c
- Distance of the closest approach of the V0 decay tracks (distance in X-Y plane between V0 decay tracks at Z_{V0}) : dca $<$ 1 cm
- Distance between the V0 decay vertex and primary vertex: path $>$ 2.0-2.5 cm (target dependent)

The invariant mass distributions of p and π^- are shown in Fig. 2 for reconstructed interactions of the 4.5 AGeV carbon beam with the C, Al, Cu, Pb targets. To extract Λ hyperon signal, the distributions were fitted to the 4-th degree Legendre polynomial (background) in the mass range 1080-1180 MeV/c^2. To avoid a bias due to possible deviation of the peak from the Gaussian shape, the numbers of Λ hyperons were determined not from the Gaussian fit but from the content of the background-subtracted histogram bins within 1107.5-1125 MeV/c^2 mass window. This mass window where Λ signal contributes was excluded from the polynomial fit. Λ signals in intervals of the transverse momentum p_T and rapidity y in the laboratory frame were reconstructed using the same fit procedure, i.e. the numbers of Λ hyperons were calculated within 1107.5-1125 MeV/c^2 window as excess signals relative to the background calculated in p_T and y intervals from fits of (p, π^-) mass spectra to the 4-th Legendre polynomial. The error of the Λ signal includes the uncertainty of the background subtraction. The Λ signals, statistical and systematic errors were calculated according to the formulae: $sig = hist - bg$, $err_{stat} = \sqrt{hist}$, $err_{syst} = \sqrt{0.5 \cdot bg}$, assuming that the background was estimated with the uncertainty of $\sqrt{0.5 \cdot bg}$. Here $hist$ and bg denote the histogram integral and the polynomial background integral within 1107.5-1125 MeV/c^2 window, respectively. If variation of the background shape due to use of the 3-th degree Legendre polynomial gave a larger uncertainty than $\sqrt{0.5 \cdot bg}$, the largest uncertainty was taken as a systematic error.

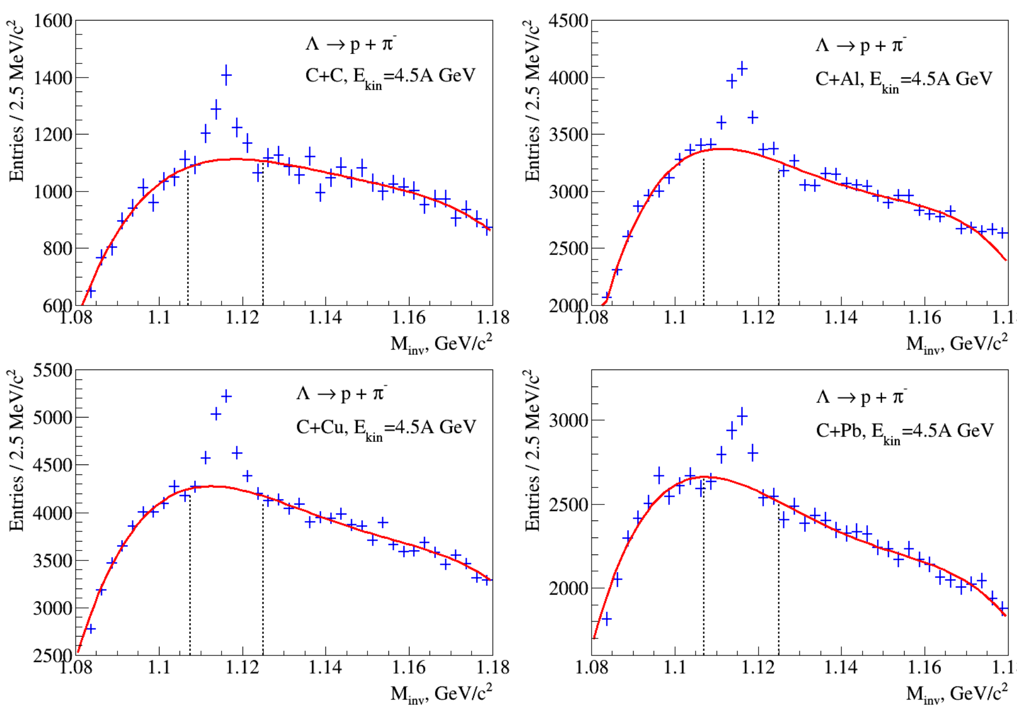

Figure 2: Invariant mass spectra of (p, π^-) pairs reconstructed in interactions of the 4.5 AGeV carbon beam with the C, Al, Cu, Pb targets. The red lines represent the polynomial fits of the background. The vertical lines show the mass window in which the Λ signal is calculated as an excess of the histogram relative to the background.

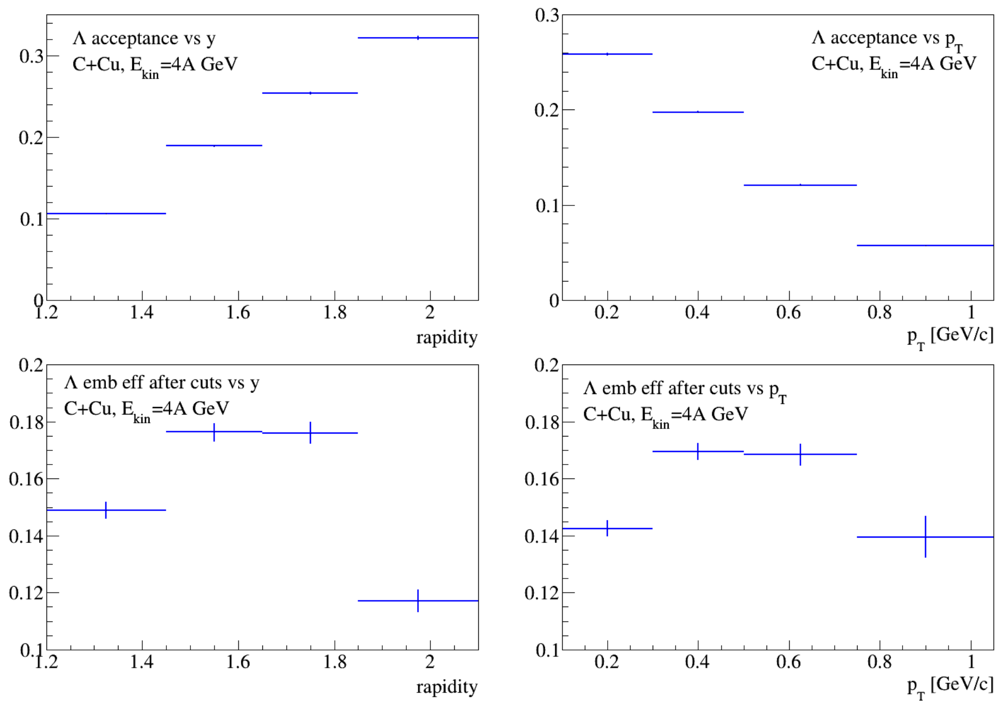

Figure 3: Λ geometrical acceptance (ϵ_{acc}) and efficiency of reconstruction of embedded Λ after applying kinematic and spatial cuts ($\epsilon_{emb+cuts}$) shown in bins of rapidity y in the laboratory frame (left plots) and in bins of p_T (right plots). Results are shown for C+Cu interactions at the 4 AGeV carbon beam energy.

4 Monte Carlo simulation

Monte Carlo event samples of C+A collisions were produced with the DCM-QGSM event generator [12, 13]. The passage of particles through the setup volume was simulated with the GEANT3 program [14] integrated into the BmnRoot software framework [15]. To properly describe the GEM detector response in the magnetic field the micro-simulation package Garfield++ [16] was used. The package gives very detailed description of the processes inside the GEM detector, including the drift and diffusion of released electrons in electric and magnetic fields and the electron multiplication in GEM foils, so that the output signal from the readout plane can be reproduced. The details of the detector alignment, Lorentz shift corrections are described in the paper [17]. To reproduce the detector effects in the reconstruction efficiency the simulated products of Λ hyperon decays

(p, π^-) were embedded into real experimental events of C+C, C+Al, C+Cu, C+Pb interactions. Simulated amplitude signals in the Forward Silicon and GEM detectors were added to amplitudes of the experimental signals in these detectors. The detector efficiencies were applied to reduce the number of hits of embedded tracks of Λ decay products. Only the Λ hyperon decay products within the tracker acceptance were used for the embedding procedure. Monte Carlo digits originated from Λ decay products were added to respective experimental events and the reconstruction was performed again for such mixed data. This allowed us to take into account many real-life effects (efficiency of tracking detectors, zero suppression, event pile-up). A fraction of successfully reconstructed embedded Λ decays after applying kinematic and spatial cuts gave the embedding and selection cuts efficiency with respect to the number of Λ hyperons decayed within the detector acceptance. The resulting Λ reconstruction efficiency is the ratio of the number of reconstructed Λ hyperons to the number of generated ones in the intervals of (y, p_T), where y is measured in the laboratory frame. The reconstruction efficiency can be decomposed into two components: $\epsilon_{rec} = \epsilon_{acc} \cdot \epsilon_{emb+cuts}$, where ϵ_{acc} stands for the geometrical acceptance of Λ hyperon decay products in the tracking detectors and $\epsilon_{emb+cuts}$ is the efficiency of reconstruction of embedded Λ after applying kinematic and spatial cuts. The obtained values of the efficiencies ϵ_{acc} and $\epsilon_{emb+cuts}$ in the y and p_T intervals are shown in Fig. 3 for 4 AGeV C+Cu interactions.

The trigger efficiency ϵ_{trig} calculated for events with reconstructed Λ hyperons is in the range between $80 \pm 2\%$ for minimum bias C+C interactions and $95 \pm 2\%$ for C+Pb interactions.

The trigger efficiency was evaluated from the trigger BD detector multiplicity distribution produced by a convolution of the multiplicity distributions for GEANT simulated events with reconstructed Λ hyperons and delta electron events from the carbon beam passage through the C, Al, Cu, Pb targets which were found to be the dominant source of delta electrons.

The systematic errors of ϵ_{trig} cover 1) the contribution of delta electrons background produced in the simulated targets with the fractional thickness from 0.5 to 1 of the real targets; 2) the spread of the trigger efficiency values calculated for different y and p_T bins of reconstructed Λ hyperons; 3) change in the trigger efficiency after adjustment (reweighting) of the simulated track multiplicity to the experimental distributions. The trigger efficiency obtained in simulation was confirmed by the analysis of data samples with the reduced trigger requirements.

5 Results

The inclusive cross section σ_Λ and yield Y_Λ of Λ hyperon production in C+C, C+Al, C+Cu, C+Pb interactions are calculated in bins of $y(\ p_T)$ according to the formulae:

$$\sigma_\Lambda(y) = \Sigma_y[N_\Lambda(y,p_T)/(\epsilon_{rec}(y,p_T)\cdot\epsilon_{trig}\cdot L)]\ , \qquad Y_\Lambda(y) = \sigma_\Lambda(y)/\sigma_{inel}$$

$$\sigma_\Lambda(p_T) = \Sigma_{p_T}[N_\Lambda(y,p_T)/(\epsilon_{rec}(y,p_T)\cdot\epsilon_{trig}\cdot L)]\ , \quad Y_\Lambda(p_T) = \sigma_\Lambda(p_T)/\sigma_{inel}$$

where L is the luminosity, N_Λ is the number of reconstructed Λ hyperons, ϵ_{rec} is the combined efficiency of the Λ hyperon reconstruction, ϵ_{trig} is the trigger efficiency, σ_{inel} is the cross section for minimum bias inelastic C+A interactions. The cross section for inelastic C+C interactions is taken from the measurement [20]. The cross sections for inelastic C+Al, C+Cu, C+Pb interactions are taken from the predictions of the DCM-QGSM model which are consistent with the results calculated by the formula: $\sigma_{inel} = \pi R_0^2(A_P^{1/3} + A_T^{1/3})^2$, where $R_0 = 1.2$ fm is an effective nucleon radius, A_P and A_T are atomic numbers of the projectile and target nucleus [23]. The uncertainties for C+Al, C+Cu, C+Pb inelastic cross sections are estimated from the alternative formula: $\sigma_{inel} = \pi R_0^2(A_P^{1/3}+A_T^{1/3}-b)^2$ with $R_0 = 1.46$ fm and $b = 1.21$ [20]. The values and uncertainties of σ_{inel} for C+C, C+Al, C+Cu, C+Pb interactions used to evaluate the Λ hyperon yields are given in Table 1.

The yields of Λ hyperons in minimum bias C+C, C+Al, C+Cu, C+Pb interactions are measured in the kinematic range on the Λ hyperon transverse momentum $0.1 < p_T < 1.05$ GeV/c and the Λ hyperon rapidity in the laboratory frame $1.2 < y < 2.1$ for 4 AGeV data ($1.25 < y < 2.15$ for 4.5 AGeV data). The systematic error of the Λ hyperon yield in every p_T and y bin is calculated as a quadratic sum of uncertainties coming from the following sources:

- Systematic errors of the embedding efficiency estimated by embedding the Λ decay products into data samples collected in different run periods.

- Systematic errors of the background subtraction under the Λ signal in the (p,π^-) invariant mass spectra as described in section 3.

- The Λ hyperon yield normalization uncertainty calculated as a quadratic sum of uncertainties of the trigger efficiency, luminosity and inelastic nucleus-nucleus cross section.

The rapidity of the beam-target nucleon-nucleon CM system calculated for an interaction of the carbon beam with the kinetic energy of 4 (4.5) GeV/nucleon with a fixed target is $y_{CM} = 1.17(1.22)$. The Λ hyperon rapidity range for 4.5 AGeV data is shifted at +0.05 to get approximately the same y^* range in the CM system as for 4 AGeV data. The transformation of the y distribution to c.m.s. gives $y^* = y - y_{CM}$. The differential spectra of the Λ hyperon yields in y are measured in the Λ hyperon transverse momentum range $0.1 < p_T < 1.05$ GeV/c. The differential y^* spectra of the Λ hyperon yields corrected for the detector acceptance and efficiency are presented in Fig. 4. The corrected differential invariant p_T spectra of Λ hyperon yields are presented in Fig. 5. The predictions of the DCM-QGSM [12, 13], UrQMD [18] and PHSD [19] models are shown for comparison. In Fig. 5 the measured invariant spectra of the Λ hyperon yields in p_T are parameterized by the form: $1/p_T d^2N/dp_T dy \propto \exp(-(m_T - m_\Lambda)/T_0)$, where $m_T = \sqrt{m_\Lambda^2 + p_T^2}$ is the transverse mass, the inverse slope parameter T_0 is a free parameter of the fit, dy corresponds to the measured y range. The values of the inverse slope T_0, extracted from the fits to the invariant p_T spectra, are summarized in Tables 1 and 2 for 4 AGeV and 4.5 AGeV carbon beam data, respectively. The value of T_0 extracted from the fit to the invariant p_T spectra measured in the carbon beam with the kinetic energy of 4 AGeV is about 95 MeV for C+C interactions rising up to 130 MeV for C+Pb interactions. The fit results are consistent within the uncertainties with the predictions of the DCM-QGSM, UrQMD and PHSD models. In general, the considered transport models describe the shape of the differential spectra on y^* and p_T, but predict more abundant yields of Λ hyperons than measured in the experiment. The UrQMD model predictions are closer to the experimental data in the normalization than the predictions of the DCM-QGSM and PHSD models. The PHSD model predicts a stronger rise of the Λ hyperon yields in the BM@N kinematic range with the atomic weight of the target than the DCM-QGSM and UrQMD models.

The measured yields of the Λ hyperons in minimum bias C+C, C+Al, C+Cu, C+Pb interactions are extrapolated to the full kinematic range using averaged predictions of the DCM-QGSM and UrQMD models. The Λ hyperon yields and cross sections in minimum bias C+C, C+Al, C+Cu, C+Pb interactions are summarized in Tables 1 and 2 and presented in Fig.6 in dependence on the kinetic energy of the carbon beam. The BM@N results are compared with the predictions of the DCM-QGSM, UrQMD and PHSD models. In general, the model predictions exceed the experimental data in the normalization. The DCM-QGSM model predicts a higher full yield of Λ hyperons than the two other models. The Λ hyperon yields and production cross sections in C+C interactions can be compared with the previous results of 23.2 ± 2.5 mb and 24 ± 6 mb measured in interactions of the carbon beam with the momentum of 4.2 GeV/c per nucleon (the beam kinetic energy of 3.36 GeV per nucleon) with the Propane Chamber experiment [21, 22], as well as with the result of the HADES experiment at 2 AGeV [23]. In Fig. 6 the BM@N results for the Λ hyperon yields in C+C minimum bias interactions are compared with the results taken from these experiments. There is a general tendency that the models predict a faster rise of the Λ hyperon yield with the energy in comparison with the experimental data.

To compare yields of particle production in nucleus-nucleus interactions, they are usually normalized to the mean number of nucleons participating in interactions (participants). The numbers of participants N_{part} in minimum bias C+C, C+Al, C+Cu, C+Pb interactions are estimated using the DCM-QGSM model. The results for N_{part} are given in Table 1. The ratios of the Λ hyperon yields to the number of nucleons-participants measured by BM@N in carbon-nucleus interactions are given in Tables 1 and 2 and compared in Fig. 7 with the predictions of the DCM-QGSM, UrQMD and PHSD models for 4 AGeV carbon nucleus interactions. The ratios measured by BM@N reach maximal values of $6.2 \cdot 10^{-3}$ and $7.6 \cdot 10^{-3}$ for C+Al interactions at the 4 and 4.5 AGeV carbon beam energy, respectively. There is a tendency that the measured ratios are smoothly decreasing for heavier target nuclei. This tendency is also predicted by the models.

6 Summary

Production of Λ hyperons in interactions of the carbon beam with the C, Al, Cu, Pb targets was studied with the BM@N detector. First physics results of the BM@N experiment are presented on the Λ hyperon yields and cross sections in minimum bias carbon-nucleus interactions at the beam kinetic energies of 4 and 4.5 AGeV. The results are compared with models of nucleus-nucleus interactions and with the results of other experiments studied carbon-carbon interactions at lower energies.

Acknowledgments. The BM@N Collaboration acknowledges support of the HybriLIT of JINR, HPC Village project and HGPU group for the computational resources provided. This work is supported by the Russian Foundation for Basic Research (RFBR) under grant No. 18-02-40036 mega.

References

[1] B. Friman, W. Nörenberg, and V.D. Toneev, Eur. Phys. J. A **3** (1998).

[2] C. Blume, J. Phys. G **31**, S57 (2005).

[3] A. Andronic *et al.*, Phys. Lett. B **695**, 203 (2011).

[4] Exploring strongly interacting matter at high densities - NICA White Paper, Eur.Phys.J. A52 (2016).

[5] BM@N Conceptual Design Report:
http://nica.jinr.ru/files/BM@N/BMN_CDR.pdf

[6] D. Baranov et al., JINST 12 (2017) no.06, C06041.

[7] M. Kapishin (for the BM@N Collaboration), Eur.Phys.J. A52 (2016) no.8, 213.

[8] M. Kapishin (for the BM@N Collaboration), Phys.Atom.Nucl. 80 (2017) no.10, 1613-1619, Yad.Fiz. 7 (2016) no.6, 543-550.

[9] M. Kapishin (for the BM@N Collaboration), Nucl.Phys. A982 (2019) 967-970.

[10] M. Kapishin (for the BM@N Collaboration), Nucl.Phys. A982 (2019) 967-970.

[11] V. Akishina and I. Kisel, J. Phys.: Conf. Ser. 599, 012024 (2015), I. Kisel, Nucl. Instrum. Meth. A **566**, 85 (2006).

[12] N. Amelin, K. Gudima, and V. Toneev, Sov.J.Nucl. Phys. 51, 1093 (1990).

[13] M. Baznat, A. Botvina, G. Musulmanbekov, V. Toneev, V. Zhezher, Phys.Part.Nucl.Lett. 17 (2020) no.3; arXiv: 1912.09277v.

[14] CERN Program Library, Long Writeup W5013, Geneva, CERN, 1993.

[15] https://git.jinr.ru/nica/bmnroot

[16] http://garfieldpp.web.cern.ch/garfieldpp

[17] D. Baranov et al., Phys.Part.Nucl.Lett. 15 (2018) no.2, 148-156.

[18] S.A. Bass *et al.*, Prog. Part. Nucl. Phys. 41 225 (1998).

[19] E.Bratkovskaya *et al.*, PSHD model

[20] H. Angelov et al., P1-80-473, JINR, Dubna.

[21] S. Arakelian et al., P1-83-354, JINR, Dubna.

[22] D. Armutlijsky et al., P1-85-220, JINR, Dubna.

[23] K. Kanaki, PhD Study of Λ hyperon production in C+C collisions at 2A GeV beam energy with the HADES spectrometer, 2007.

Table 1: Λ hyperon yields, cross sections and p_T spectra slope parameters in minimum bias 4 AGeV C+C, C+Al, C+Cu, C+Pb interactions. The first error given is statistical, the second error is systematic.

4 AGeV Carbon beam	C+C	C+Al	C+Cu	C+Pb
Measured Λ yield $/10^{-2}$	$1.64 \pm 0.13 \pm 0.10$	$2.86 \pm 0.25 \pm 0.20$	$3.07 \pm 0.2 \pm 0.16$	$3.66 \pm 0.48 \pm 0.36$
Full Λ yield N_Λ $/10^{-2}$	$4.53 \pm 0.36 \pm 0.27$	$8.82 \pm 0.77 \pm 0.60$	$13.1 \pm 0.9 \pm 0.7$	$22.6 \pm 3.0 \pm 2.3$
N_{part}, DCM-QGSM	9.0	13.4	23.0	50.5
$N_\Lambda/N_{part}/10^{-3}$	$5.03 \pm 0.40 \pm 0.30$	$6.58 \pm 0.57 \pm 0.45$	$5.70 \pm 0.39 \pm 0.30$	$4.48 \pm 0.59 \pm 0.46$
Λ cross section, mb	$37.6 \pm 3.0 \pm 2.3$	$111.2 \pm 9.7 \pm 7.6$	$234 \pm 16 \pm 12$	$695 \pm 91 \pm 72$
σ_{inel}, mb	830 ± 50 [20]	1250 ± 50 [23]	1790 ± 50 [23]	3075 ± 50 [23]
Inverse slope T_0, MeV	$95 \pm 11 \pm 9$	$119 \pm 15 \pm 12$	$125 \pm 11 \pm 9$	$125 \pm 25 \pm 21$

Table 2: Λ hyperon yields, cross sections and p_T spectra slope parameters in minimum bias 4.5 AGeV C+C, C+Al, C+Cu, C+Pb interactions. The first error given is statistical, the second error is systematic.

4.5 AGeV Carbon beam	C+C	C+Al	C+Cu	C+Pb
Measured Λ yield$/10^{-2}$	$2.24 \pm 0.26 \pm 0.19$	$3.55 \pm 0.34 \pm 0.26$	$4.06 \pm 0.32 \pm 0.26$	$4.00 \pm 0.57 \pm 0.43$
Full Λ yield $N_\Lambda/10^{-2}$	$5.54 \pm 0.64 \pm 0.47$	$10.9 \pm 1.0 \pm 0.8$	$16.4 \pm 1.3 \pm 1.1$	$27.3 \pm 3.8 \pm 2.9$
$N_\Lambda/N_{part}/10^{-3}$	$6.16 \pm 0.71 \pm 0.52$	$8.13 \pm 0.75 \pm 0.60$	$7.13 \pm 0.56 \pm 0.48$	$5.41 \pm 0.75 \pm 0.57$
Λ cross section, mb	$46.0 \pm 5.3 \pm 3.9$	$137 \pm 13 \pm 10$	$293 \pm 23 \pm 19$	$839 \pm 117 \pm 90$
Inverse slope T_0, MeV	$114 \pm 16 \pm 12$	$137 \pm 19 \pm 15$	$122 \pm 13 \pm 11$	$129 \pm 24 \pm 19$

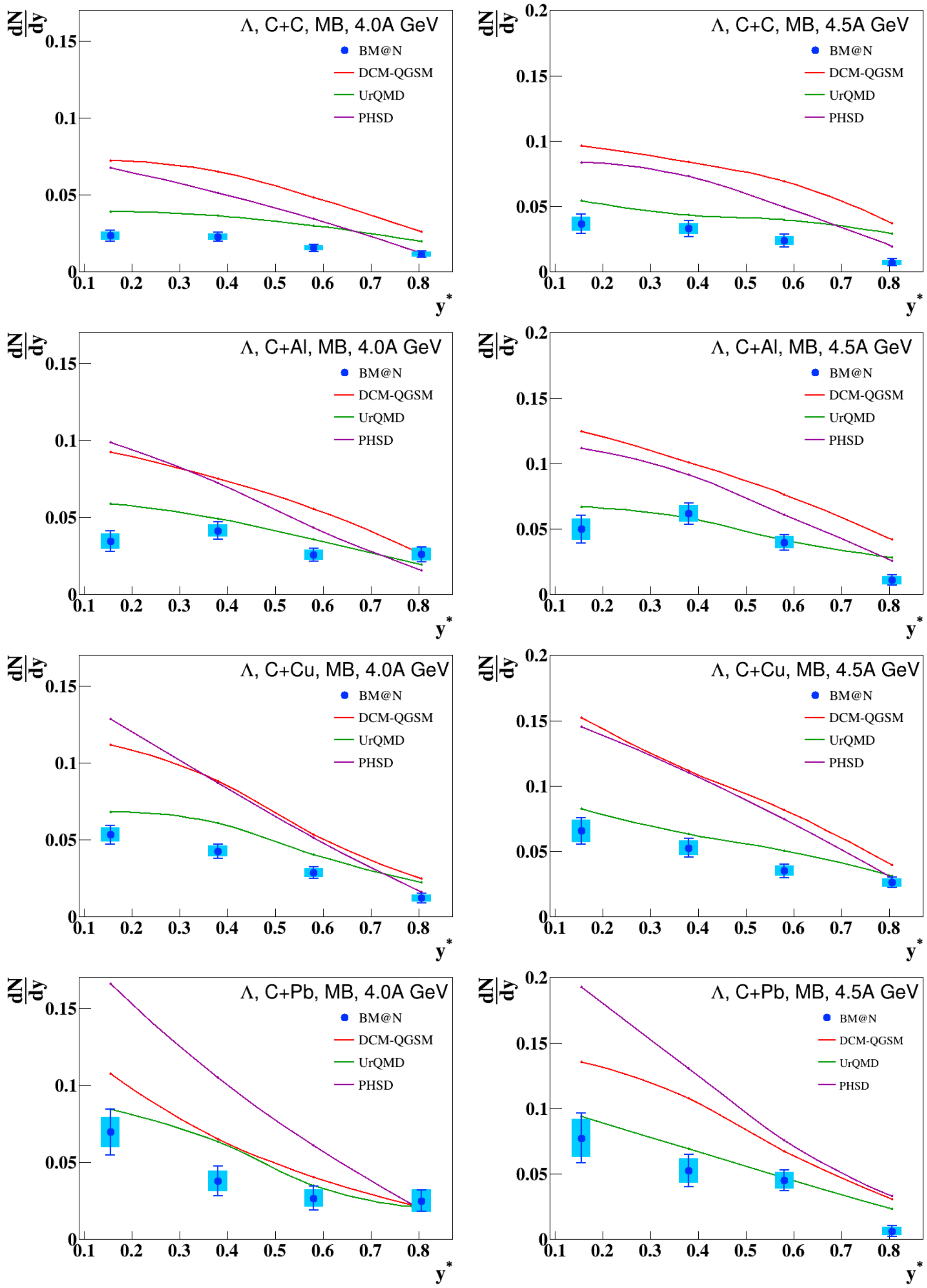

Figure 4: Rapidity y^* spectra of Λ hyperons produced in minimum bias C+C, C+Al, C+Cu, C+Pb interactions with the carbon beam energy of 4 AGeV (left plots) and 4.5 AGeV (right plots). The error bars represent the statistical errors, the blue boxes show the systematic errors. The predictions of the DCM-QGSM, UrQMD and PHSD models are shown as colored lines.

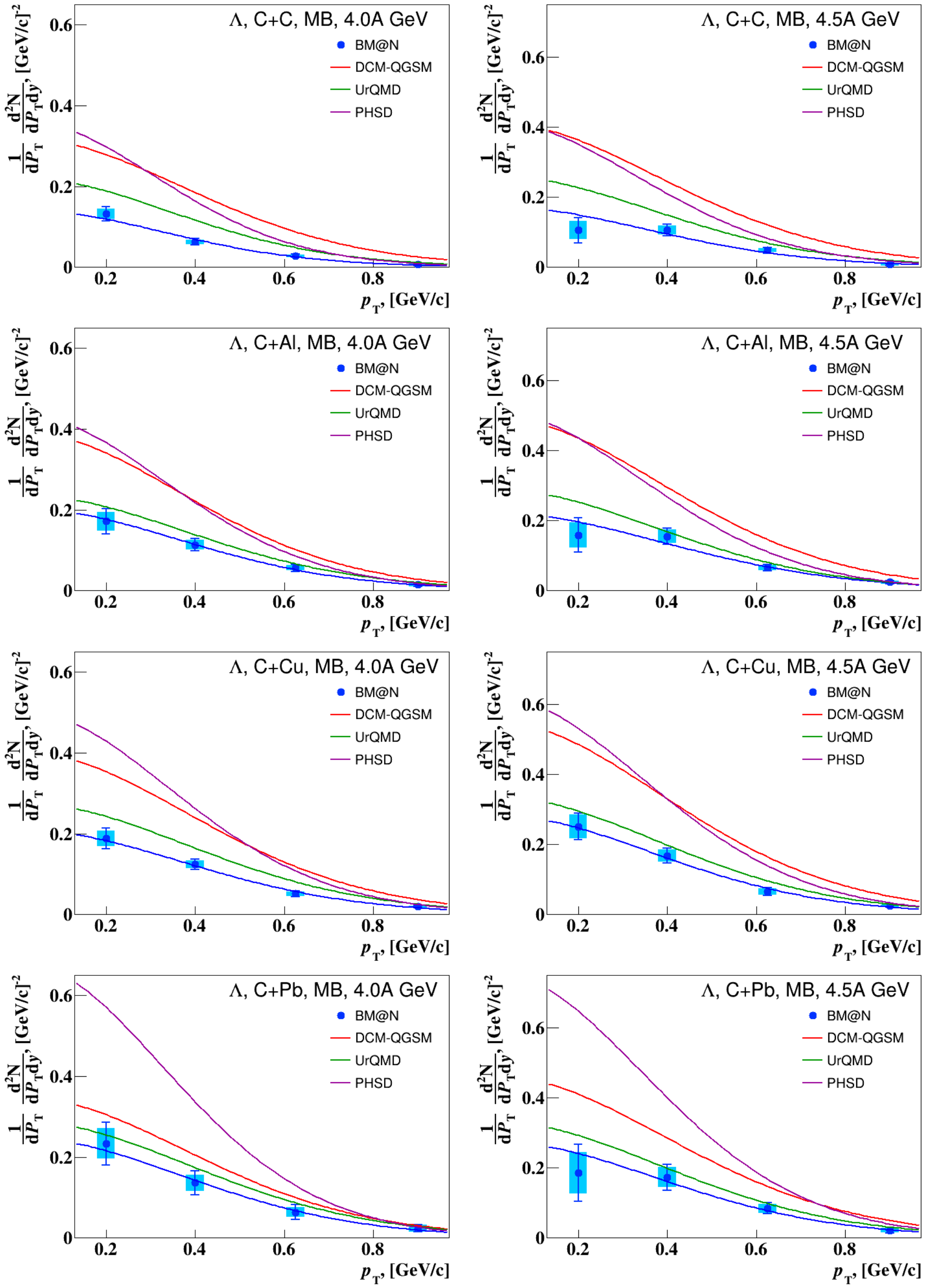

Figure 5: Transverse momentum p_T spectra of Λ hyperons produced in minimum bias C+C, C+Al, C+Cu, C+Pb interactions with the carbon beam energy of 4 AGeV (left plots) and 4.5 AGeV (right plots) The error bars represent the statistical errors, the blue boxes show the systematic errors. The blue lines represent the results of the parameterization described in the text. The predictions of the DCM-QGSM, UrQMD and PHSD models are shown as colored lines.

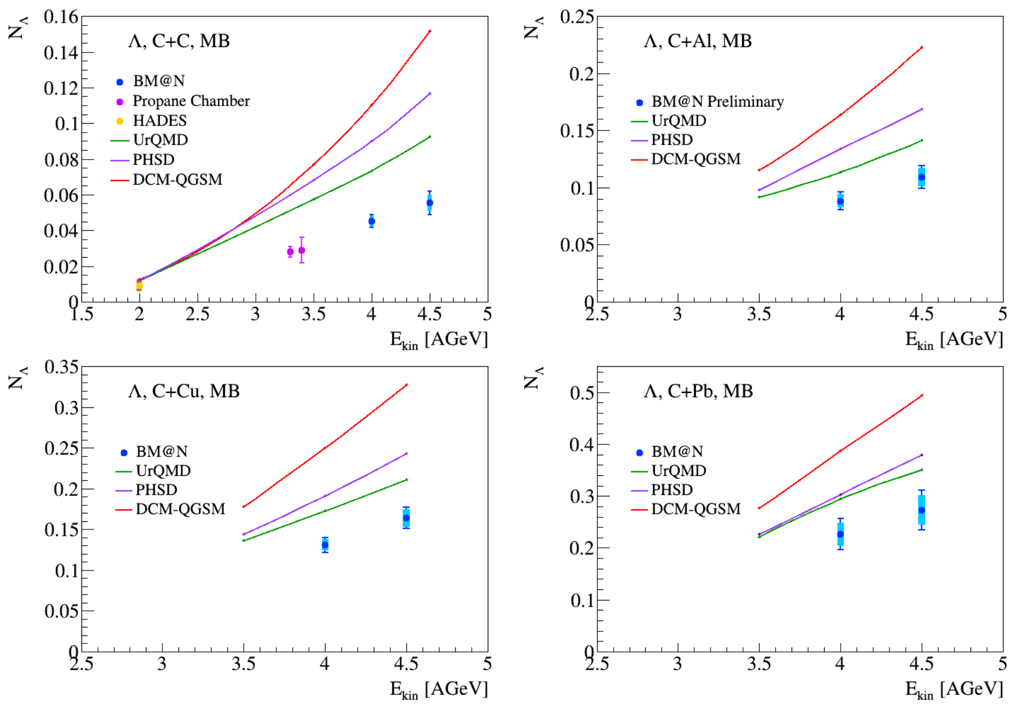

Figure 6: Energy dependence of Λ hyperon yields in minimum bias C+C, C+Al, C+Cu, C+Pb interactions. The BM@N error bars represent the statistical errors, the blue boxes show the systematic errors. The BM@N results for C+C interactions are compared with the experimental data taken from [21–23]. The predictions of the DCM-QGSM, UrQMD and PHSD models are shown as colored lines.

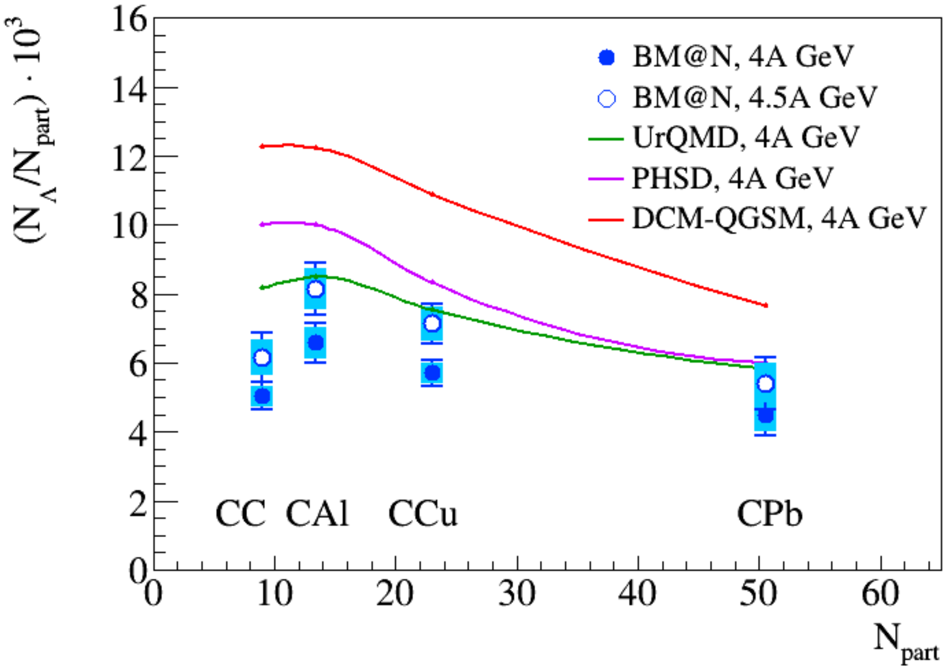

Figure 7: Ratios of the Λ hyperon yields to the number of nucleons-participants measured by BM@N in minimum bias carbon-nucleus interactions at 4 and 4.5 AGeV. The error bars represent the statistical errors, the blue boxes show the systematic errors. The predictions of the DCM-QGSM, UrQMD and PHSD models for 4 AGeV carbon-nucleus interactions are shown as colored lines.